Journal of Advanced Research in Applied Sciences and Engineering Technology

Journal homepage:
https://semarakilmu.com.my/journals/index.php/applied_sciences_eng_tech/index
ISSN: 2462-1943

The Effect of an Aluminium Disc Rotator on Polyvinyl Chloride (PVC) Material using 360° Lateral Sliding Disc Triboelectric Generator (TEG)

Muhammad Mahfuz Salehhon[1,*], Zul Izie Hafifi Mohamad Ghazali[1], Ahmad Nazirul Manan[1], Nur Farahana Mat Isa[1], Nur Aisyah Mohd Yusri[1], Hafizal Yahaya[1], Rasli Abd Ghani[1], Fauzan Ahmad[1]

[1] Malaysia–Japan International Institute of Technology (MJIIT), Universiti Teknologi Malaysia, Jalan Sultan Yahya Petra, 54100 Kuala Lumpur, Malaysia

ARTICLE INFO

Article history:
Received 2 May 2023
Received in revised form 10 July 2023
Accepted 6 September 2023
Available online 28 November 2023

Keywords:
Lateral sliding; triboelectric effect; rotating speed

ABSTRACT

Triboelectric generators have the ability to harvest energy from human activities, mechanical vibration, and other sources to drive minor electronic devices. In many circumstances, charges created from a triboelectric process are referred to as a negative effect or waste energy. Here, this paper will demonstrate an approach of the charging process in friction with a rotator and stator to investigate the effects of rotating speed and the different thickness of electrification to the output voltage. The 360° lateral sliding disc triboelectric generator (TEG) fabricated by connecting an Aluminium disc to the motor as a rotator, while a Polyvinyl Chloride (PVC) sheet placed at the top of an acrylic coated by a copper electrode served as a stator. PVC material with different thicknesses (0.2, 0.5 and 0.7 mm) and grit sizes were used (P500, P1000 and P1500) and prepared prior to the experiment. Thus, three different rotational speeds (500, 1000 and 1500 rpm) were monitored using a tachometer to standardize the speed for each set of experiment. Such as a TEG at 1500 rpm on a 0.2 mm thick sample with P500 grit size modification delivers a maximum voltage output, V_{RMS} of 13.8 mV, with the maximum calculated current of 69 µA and the maximum power density of 0.485 mW/m^2.

1. Introduction

A severe energy crisis may be a major factor limiting the quality of life. Even so, maintaining energy derived from natural resources remains one of humanity's biggest challenges [1]. By 2022, there will be 7.9 billion people on the planet, which will result in a rise in demand for power generation that is more efficient and produces fewer emissions [2]. The most effective way to reduce greenhouse gas emissions might be to introduce sustainable, new, and renewable energy [3]. Nanotechnology-based energy harvesting, and conversion devices have lately attracted more attention since they are projected to be essential for creating and operating self-powered nanodevices and nanosystems [4-10].

* *Corresponding author.*
E-mail address: mahfuzsalehhon@gmail.com (Muhammad Mahfuz Salehhon)

https://doi.org/10.37934/araset.34.1.187198

In general, materials properties can be modified to fit the anticipated component application by altering their chemistries and processing [10]. The first piezoelectric nanogenerator that effectively converted mechanical energy into electricity was shown in 2006 by a team from the School of Material Science and Engineering at Georgia Institute of Technology [11]. In contrast, triboelectric associated electrostatic phenomena are most prevalent in our daily lives, from walking to driving, but they haven't been considered as an energy source for electricity. It would be fantastic if one could produce electricity using the electric charges or potential created by a tribological process. In these circumstances, a 2012 invention known as a triboelectric generator (TEG), which converts mechanical energy to electrical energy by frictional contacts between two different polarities of material, serves as a viable solution and plays a crucial role in the development of environmentally friendly energy sources [12].

In 2018, a team of researchers from the University of Surrey's Advanced Technology Institute provided an in-depth, detailed, and clear view of TEG due to its capacity to power Internet of Things (IoT) devices, wearable devices, and self-powered electronic applications. According to research, a TEG can produce 0.22 mW/m^2, which is enough to illuminate 48 light-emitting diodes (LEDs) [13]. In order to unlock the full potential of the TEG system, it makes sense to modify the material used to improve the energy generated. The power output of the TEG was influenced by several factors, including the material, shape, size, and motion input [14-17].

The purpose of this paper was to explore the effect of regulating the rotating speed of an aluminium disc with varied thicknesses and surface roughness of a polyvinyl chloride (PVC) on the electrical power generation using 360° Lateral Sliding Disc TEG's system. Aluminium occupies a high rank in the triboelectric series as a positive triboelectric material with a strong electron donor property, while PVC occupies a lower rank as a negative triboelectric material because of its high electron acceptor property. The transmission of charge increases with the distance between these two materials in a triboelectric series, increasing the theoretical possibility of producing more power. (PVC), a type of plastic material, is one of the most widely used and produced [18]. This is due in large part to PVC's favourable mechanical properties, high chemical resistance, and resistance to water and environmental elements, in addition to its low production costs [19]. Consequently, a summarized conclusion and some remarks pertaining to the findings are established. This work provides an excellent opportunity to interrogate TEG's potential as new energy technology from a material's point of view.

2. Experimental Details

The 360° lateral sliding disc TEG required a single pattern rotator and two layers of stator to operate. The rotator in this case shown in Figure 1(a) is made up of 10 radially arrayed aluminium disc that is rotated by a DC motor. The stator shown in Figure 1(b) is constructed of an acrylic with a copper foil on top with 10 separated gaps in between as an electrode. The system must have this rotator-stator complementary pattern in order to produce AC output. While the bottom part of an acrylic disc served as an insulator, preventing any electron loss from the device. Lastly, the PVC sheet material used in this study acts as an electrification layer of TEG.

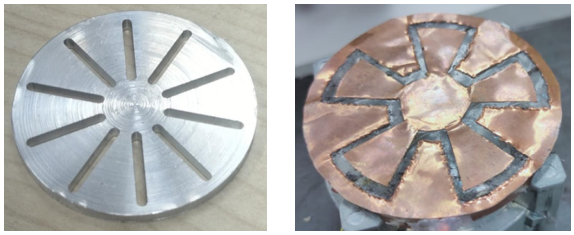

(a) (b)

Fig. 1. (a) 10 radially arrayed aluminium disc (rotator), (b) Copper foil Electrode with an acrylic base (stator)

The 2D illustration of 360° lateral sliding disc TEG setup was shown in Figure 2 equipped with DC power supply to rotate DC motor attached with an aluminium rotator. The DC motor and all of the rotator parts were then gravity-released toward the PVC sheet at the top of the stator throughout the experiment. This ensures that constant pressure is applied to each PVC sheet, thereby minimising the gap between them. Then, the aluminium rotator will frictionally rotate above various static PVC sheets. Two lead wires are used as the positive and negative connections and are linked in parallel with a load resistor to transfer the generated power signal from the copper electrode to the oscilloscope. Thus, a Tektronix DPO2002B oscilloscope was used to measure the voltage output and display the signal while the current and power density were calculated across a 220 Ω resistor acting as a dummy load.

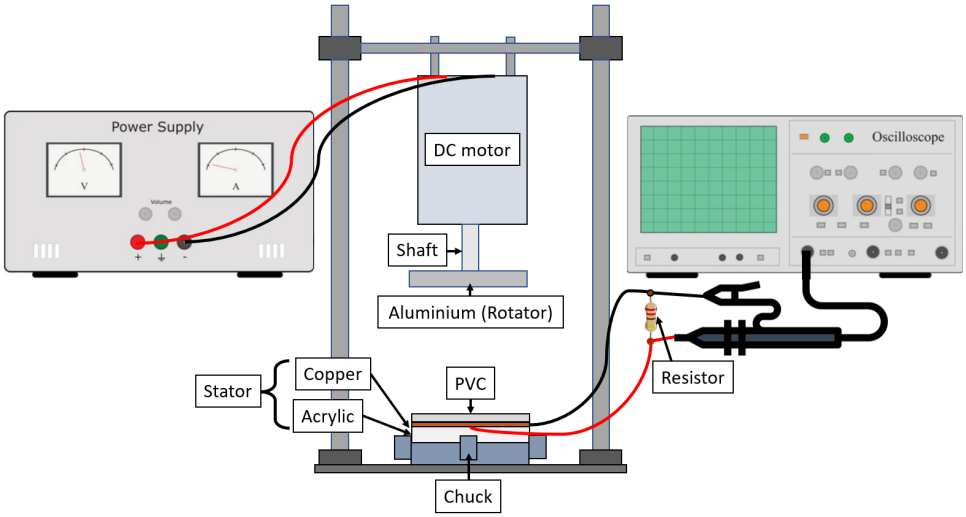

Fig. 2. 360° Lateral Sliding Disc TEG Setup

Prior to the experiment, surface modification was performed using sandpaper on PVC materials with three different thicknesses, 0.2, 0.5, and 0.7 mm. According to a previous study conducted at Donghua University in Shanghai, the ideal thickness rises from 0.5 mm to 0.7 mm [20]. Therefore, the purpose of this study was to determine whether or not the ideal thickness could be as low as 0.2 mm. Sandpaper with P500, P1000 and P1500 grit sizes were used to differentiate as sample for each set of experiment and rubbed 50 times in a row in one direction with constant pressure. Due to closer contact and more sufficient friction, large grit sizes (above 2000) were used in a prior study conducted in 2017 [21]. However, in this instance, different P500 levels for each grit size were used to examine the effects of the lower grit sizes. The grit size shows that the lower the number of P, the rougher the sandpaper's surface. Following that, isopropyl alcohol was used to clean each sample of PVC. The

roughness measurement values, Ra of the sample was determined using the SJ-310 Mitutoyo Surface Roughness Tester before and after running the experiment. The roughness of PVC is constant at 0.169 µm when purchased. As a result, its roughness increases accordingly upon rubbing with sandpaper following the grit size numbers as described.

The Royal Society of Chemistry reported in research from 2021 that the TEG can effectively recycle spinning mechanical energy to power various electrical devices at an impressively high rotational speed of 7500 rpm [22]. In this experiment, substantially lower rotational speeds were tested, ranging from 500 to 1500 rpm, to see if TEG could still provide adequate power. Therefore, three different rotational speeds; 500, 1000, and 1500 rpm have been used as parameters in this study. These speeds were measured by the mini non-contact tachometer UT373. A DC power supply was used to run the DC motor that was attached to the rotator, and it was able to regulate the input voltage and current to achieve the specified rotational speed values. As a result, Table 1 below contains a list of the 27 PVC sheet samples tested.

Table 1
Sample list of PVC

Sample Thickness (mm)	Rotational Speed (RPM)	Grit Size (P)
0.2	500	P500
		P1000
		P1500
	1000	P500
		P1000
		P1500
	1500	P500
		P1000
		P1500
0.5	500	P500
		P1000
		P1500
	1000	P500
		P1000
		P1500
	1500	P500
		P1000
		P1500
0.7	500	P500
		P1000
		P1500
	1000	P500
		P1000
		P1500
	1500	P500
		P1000
		P1500

3. Results and Discussion

3.1 Effect of Grit Size on Voltage Output, V_{RMS}

Figure 3(a) to Figure 3(c) depict the impact of grit sizes on voltage output, V_{RMS}, at different sample thicknesses. The grit size used in this work determines the surface roughness of the sample. The greater the number of grit sizes, the smoother the surface material. According to Figure 3(a), the pattern exhibits a drop in V_{RMS} of 20.1% when the sample's thickness is 0.2 mm, going from 12 mV at P500 to 9.81 mV at P1000 and 9.2% to 8.83 mV at P1500. This pattern resembled a 0.5 mm thickness sample's voltage output, which drops sharply from 11.8 mV at P500 to 9.76 mV at P1000 by 18.9% before decreasing by 9.6% to 8.87 mV at P1500. This demonstrates that the voltage output value for each grit size is slightly lower at 0.5 mm thickness than at 0.2 mm thickness. After the sample's thickness was increased to 0.7 mm, the V_{RMS} steadily dropped from 10.7 mV at P500 to 8.63 mV at P1500, a drop of 11.7% and then 9.8%.

Meanwhile, Figure 3(b), which portrays the intermediate speed of rotation at 1000 rpm and a pattern with 0.5 mm and 0.7 mm thickness for P1000 grit size, reveals a very distinct pattern. When the sample's thickness is 0.7 mm, the V_{RMS} increased by 0.1% from 9.95 mV at P500 to 9.96 mV at P1000 before decreasing by 9.2% to 9.08 mV at P1500. While V_{RMS} continues to be 11.4 mV at P500 and P1000 before abruptly falling to 9.28 mV at P1500 by 20.5%. In other words, the findings for 0.5 mm and 0.7 mm are pretty consistent across P500 and P1000, maybe because the effect for both grit sizes is comparable in this scenario. This might be due to unforeseen noise, which is an essential factor to consider before doing the experiment. In Figure 3(b), where the sample size is 0.2 mm, displays a similar trend to Figure 3(a). The V_{RMS} decreases dramatically, by 17.2%, from 12.6 mV at P500 to 10.6 mV at P1000, subsequently falling by 9.7% to 9.62 mV at P1500.

Figure 3(c) illustrates three distinct drop styles ranging from P500 to P1000. V_{RMS} drops by 18.2% from 13.8 mV, which is the highest V_{RMS} value to 11.5 mV when the sample is 0.2 mm thick. When the sample was enlarged to 0.5 mm, the V_{RMS} reduced by 6.7% from 12 mV to 11.2 mV. However, the V_{RMS} drops by 0.9% from 11.3 mV to 11 mV with 0.7 mm thickness, and this trend is nearly identical from P1000 to P1500 for 0.2 mm and 0.5 mm thickness' samples. At 0.2 mm thick, the V_{RMS} declined by 2.6% from 11.5 mV to 11.2 mV, and at 0.5 mm thick, it reduced by 2.7% from 11.2 mV to 10.9 mV. The V_{RMS} decreased by 13.2% from 11 mV at P1000 to 9.64 mV at P1500 when the sample was 0.7 mm thick.

The graph's overall pattern demonstrates that V_{RMS} will rise as the number of grit sizes operated declines. The reason for this is that as the grit size reduces, the material surface area and surface roughness both increases. Greater surface contact will occur during the rotation of the aluminium rotator toward the PVC material due to the material's wide surface area and high surface roughness. The frictional force generated during rotation will rise under these circumstances, leading to a greater output voltage [23,24]. More surface modification will be required for future investigations to grasp this property, in depth.

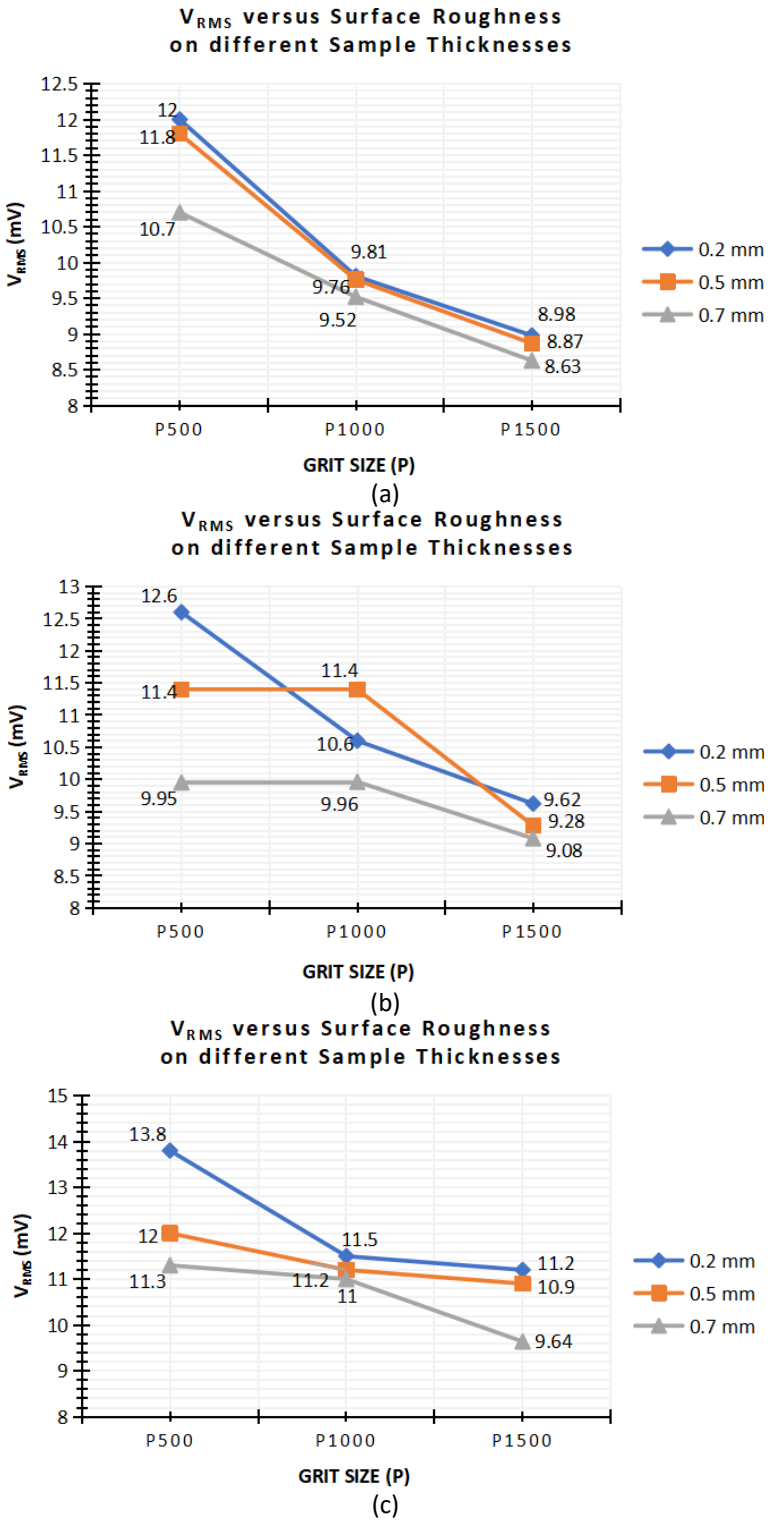

Fig. 3. The voltage output with different grit sizes and thicknesses at (a) 500 rpm, (b) 1000 rpm and (c) 1500 rpm

3.2 Effect of RPM on Current

Figure 4(a) to Figure 4(c) showed how changing the rotation speed, or rpm, affected the current at different grit sizes. When the sample is made up of P500 and P1000 grit grades, Figure 4(a) demonstrates that the current increased continuously. The current's increment is 4.9% and 7.6% with P500 and 9.1% and 8.1% with P1000, respectively, from 60 µA and 49.1 µA at 500 rpm to 69 µA,

which is the highest current output, and 57.5 µA at 1500 rpm. The current climbed by 6.9% from 44.9 µA at 500 rpm to 48.1 µA at 1000 rpm before rising even higher by 15.2% to 56 µA at 1500 rpm when the sample is made up of P1500 grit grade.

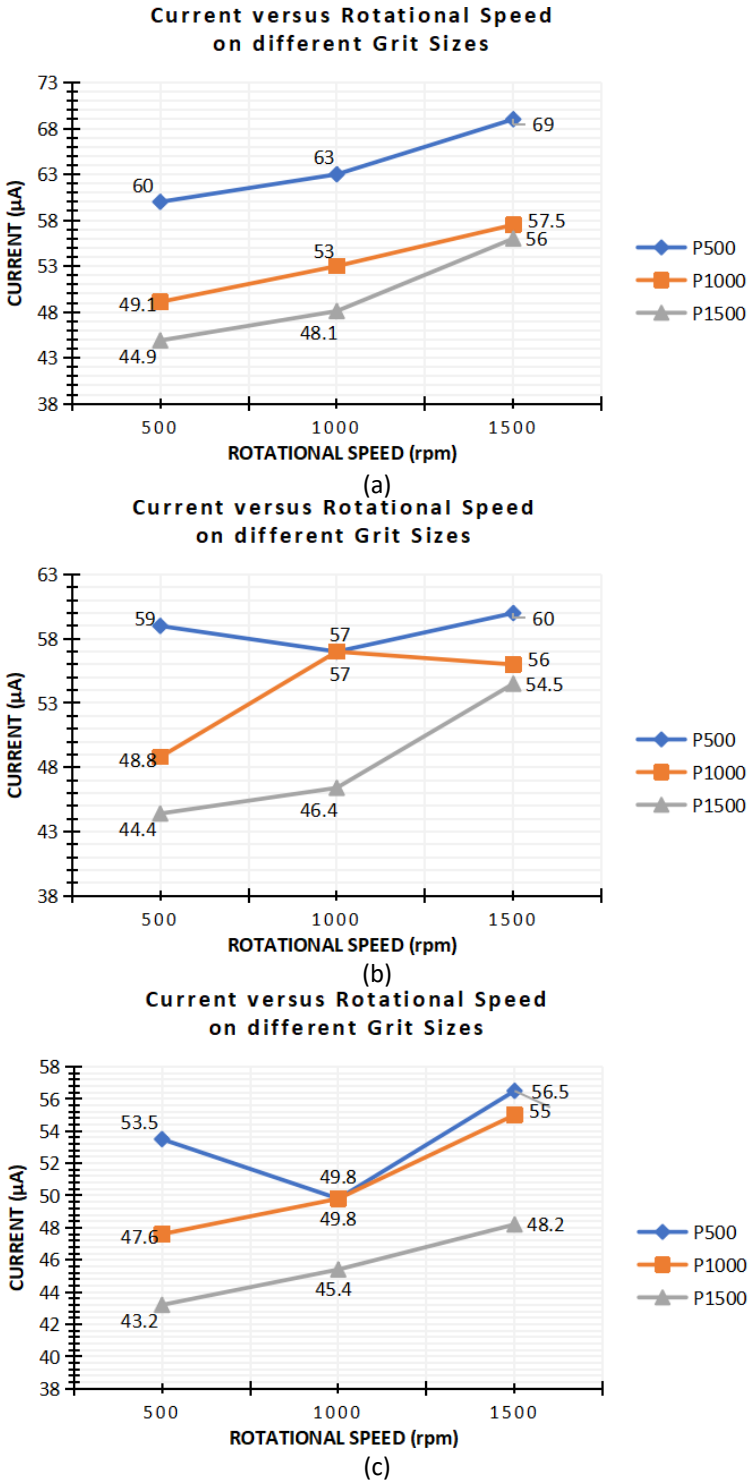

Fig. 4. The current at different rotational speeds and grits with (a) 0.2 mm, (b) 0.5 mm, and (c) 0.7 mm sample thickness

According to Figure 4(b), the current changed from 59 µA with P500 and 48.8 µA with P1000 at 500 rpm to 57 µA at 1000 rpm, a decrease of 3.4%, and an increase of 15.5%. The current, however, returned by 5.1% to 60 µA with P500 and slightly decreased by 1.8% to 56 µA with P1000. The pattern

is quite similar to Figure 4(a) when utilizing a sample with a P1500 grit size. In that figure, the current increased by 4.4% from 44.4 µA at 500 rpm to 46.4 µA at 1000 rpm, and subsequently increased by 16.1% further until it reached 54.5 µA at 1500 rpm.

Figure 4(c) illustrates a similar trend to Figure 4 for the sample at 500 and 1000 rpm, where the current reduced from 53.5 µA by 7.2% with P500 and climbed from 47.6 µA by 4.5% with P1000 to 49.8 µA, except at 1500 rpm, both grit sizes increased to 56.5 µA by 12.6% and 55 µA by 9.9%. When the sample's grit size was raised to P1500, the current climbed continuously by 5% and 6% from 43.2 µA at 500 rpm to 48.2 µA at 1500 rpm, respectively.

Figure 4(b) and Figure 4(c), which deviated from Figure 4(b), revealed that P500 and P1000 reported very similar values at 1000 rpm. As previously said, this may be because the grit sizes in this scenario are comparable. To obtain better results in comparison, more substantial differences in grit size need to be studied. Generally, a higher rotational speed has a bigger impact on the voltage output and results in better performance compared to a lower rotational speed. This materializes as a higher rpm leads to an increase in friction between two surfaces made of triboelectric material, resulting in heat and higher charge generation in the system [22]. As stated earlier, higher rotational speeds result in higher voltage generation, which can serve as the foundation for further studies on extremely high rpm values.

3.3 Effect of Sample Thickness on Calculated Power Density

Figure 5(a) to Figure 5(c) demonstrate the impact those sample thicknesses had on the output power density results calculated at various rotating speeds. Figure 5(a) shows that when the sample was rotated at 1500 rpm, the power density decreased by 27.7%, from 0.485 mW/m^2 the highest output power density with 0.2 mm thickness to 0.367 mW/m^2 with 0.5 mm thickness, before decreasing by 12.1% to 0.325 mW/m^2 with 0.7 mm thickness. When the sample reduced the spin to 1000 rpm, the power density dropped by 19.9% and 27.1%, from 0.404 mW/m^2 with 0.2 mm thickness to 0.252 mW/m^2 with 0.7 mm thickness, respectively. The power density however, only marginally decrease from 0.367 mW/m^2 with 0.2 mm thickness to 0.355 mW/m^2 by 3.3% with 0.5 mm thickness, while it decreased to 0.292 mW/m^2 with 0.7 mm thickness by 19.5% when the sample rotated at 500 rpm.

Figure 5(b) shows that the power density continuously fell from 0.245 mW/m^2 and 0.337 mW/m^2 with 0.2 mm thickness to 0.231 mW/m^2 and 0.308 mW/m^2 with 0.7 mm thickness as the rotation speed increased from 500 rpm to 1500 rpm. The drop was 0.8% and 5.1% for 500 rpm and 5.5% and 3.5% for 1500 rpm, respectively. The power density, however, increased significantly by 14.6% from 0.286 mW with 0.2 mm thickness to 0.331 mW/m^2 with 0.5 mm thickness before falling by 26.7% to 0.253 mW/m^2 with 0.7 mm thickness.

Figure 5(c) shows that when the rotational speed is increased to 1500 rpm, the power density decreases by 5.1% from 0.319 mW/m^2 with 0.2 mm thickness to 0.303 mW/m^2 with 0.5 mm thickness before dropping significantly by 24.4% to 0.237 mW/m^2 with 0.7 mm thickness. In contrast, the patterns of the other two rotational speeds were comparable. At 1000 rpm, the power density dropped from 0.236 mW/m^2 with 0.2 mm thickness to 0.219 mW/m^2 with 0.7 mm thickness, a 7.5% and 4.2% decrease, respectively. The power density decreased by 2.5% and 5.1%, respectively, from 0.205 mW/m^2 with 0.2 mm thickness to 0.19 mW/m^2 with 0.7 mm thickness at the lowest rotational speed of 500 rpm.

The power density that may be generated evidently rose along with sample thickness. This is most likely due to the thinner sample providing a better medium for electron transit, allowing it to pass through the electrification layer more effectively [20,25]. As a result, a sample with a lower thickness

yields more power density than a sample with a higher thickness. To optimize the power generated, future studies should retain the thickness to as low as possible.

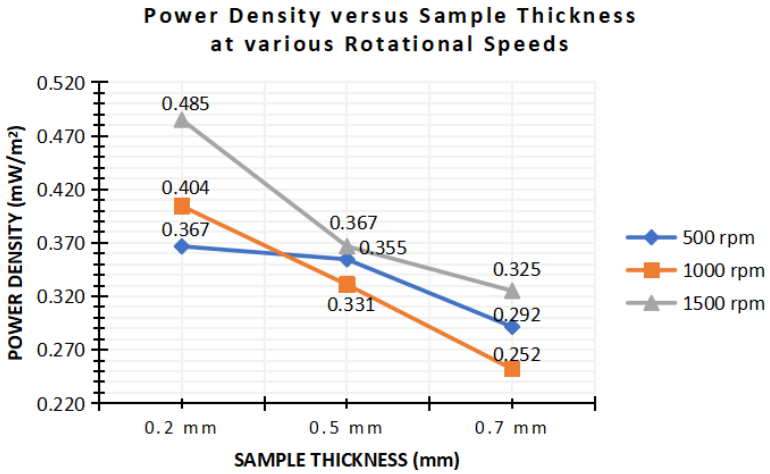

(a)

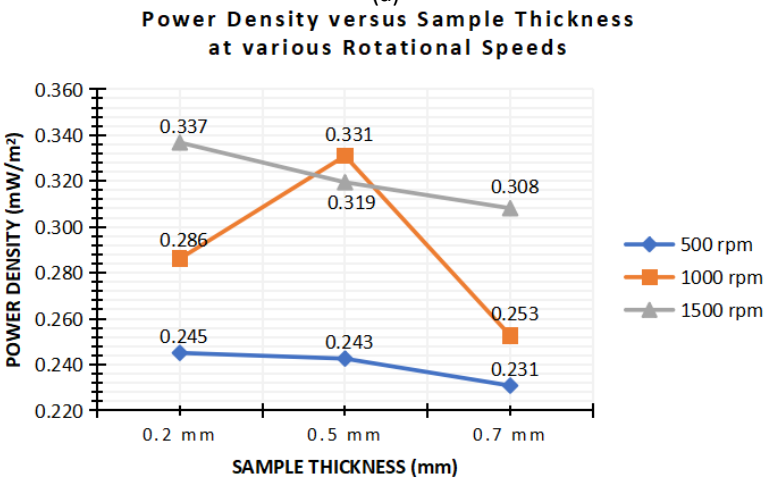

(b)

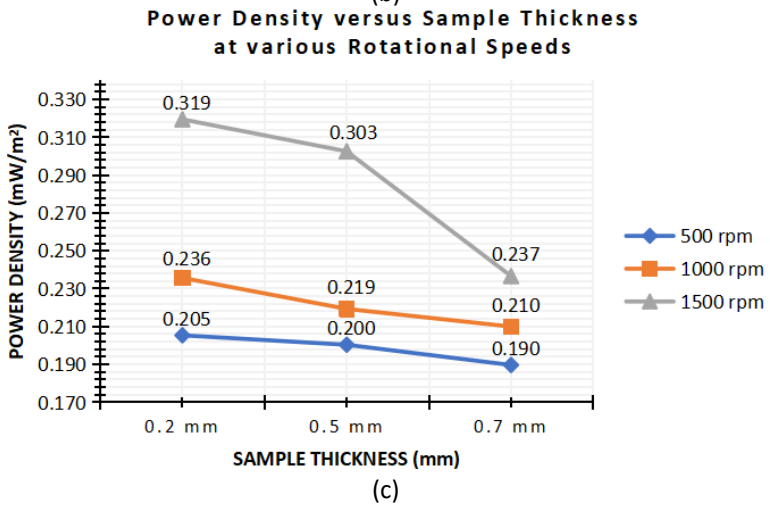

(c)

Fig. 5. The power density at different sample thicknesses and rotational speeds with (a) P500, (b) P1000, and (c) P1500 grit size

3.4 Effect of Rotation on Line Roughness Sample, Ra

Table 2 reveals the influence of rotation on the value of line roughness before and after the experiment, Ra. Ra is at the greatest before the experiment at P500, followed by P1000, and the lowest at P1500. In other words, the grit size is inversely related to the line roughness. The rougher the surface material, the higher the line roughness. At 500 rpm, Ra for the sample with P500 grit size decreased by 80.3%. The percentage reduced for each sample were 98.6% at 1000 rpm and 105.1% at 1500 rpm. Ra decreased by 38.8%, 101.1%, and 132.4% at 500, 1000, and 1500 rpm, respectively when the sample's grit size was at P1000. Ra decreased with P1500 at 500 rpm by 62%. At 1000 and 1500 rpm, the subsequent down drifts were 73.3% and 69.7%, respectively. This shown that the Ra dropped for P1500 was the least compared to P500 and P1000 because the initial roughness was already low, therefore the effect of the rotation was less pronounced than it would have been for a surface with a greater beginning roughness.

Table 2
Line Roughness value, Ra before and after the experiment

Grit Size (P)	Rotational Speed (RPM)	Ra Before (µm)	Ra After (µm)
P500	500	0.881	0.376
	1000		0.299
	1500		0.274
P1000	500	0.536	0.362
	1000		0.176
	1500		0.109
P1500	500	0.205	0.108
	1000		0.095
	1500		0.099

In general, the Ra is entirely influenced by the grit sizes and rpm values. The larger value of grit size, decreased a much smaller proportion of Ra as the material is closer to the smooth surface state, which translates to the material losing its roughness after each rotation. This might be because the rotator disc, which has no surface modification, exerted force on the electrification layer during rotation, causing the material to revert to its natural state before any change was undertaken. Furthermore, the relationship between rpm and the time required must be studied for future work in order to sustain the output power of the generator itself for a longer period.

4. Conclusions

In summary, the effects on electrical power generation were successfully investigated when the TEG system was tested with different grit sizes (P500, P1000, and P1500), different sample thicknesses of PVC (0.2, 0.5, and 0.7 mm) and different rotational speeds of an Aluminium disc (500, 1000, and 1500 rpm). TEG at 1500 rpm on a 0.2 mm thick sample with P500 grit size modification delivers a maximum voltage output, V_{RMS} of 13.8 mV, with the maximum calculated current of 69 µA and the maximum power density of 0.485 mW/m^2. The analysis of rotational speed parameters produced the best overall findings, with the difference between each rpm having a larger significant value.

It is distinctly clear from this research that at lower grit sizes (rougher surface), higher rotational speeds and with thinner samples, the electrification frequency between the PVC and Aluminium interface significantly increases, leading to higher output voltages and subsequently improves the

power density. However, further advancements in increasing polymer conductivity should be considered in order to generate more power density. Additionally, it is advised to keep the thickness low while increasing the surface roughness with a higher Ra value and a faster rotating speed (rpm) for future advancement. The level of electrical output generated makes TEG a very significant choice for future small devices' power sources.

Acknowledgment
The authors would like to thank the Japanese Chamber of Trade and Industry, Malaysia (JACTIM), Malaysia-Japan International Institute of Technology (MJIIT) Covid-19 Research Proposal Competition 2021 for funding this research.

References

[1] Adnan, Nur Fatimah, Kee Quen Lee, Hooi Siang Kang, Keng Yinn Wong, and Hui Yi Tan. "Preliminary investigation on the energy harvesting of vortex-induced vibration with the use of magnet." *Progress in Energy and Environment* 21 (2022): 1-7. https://doi.org/10.37934/progee.21.1.17

[2] Gielen, Dolf, Francisco Boshell, Deger Saygin, Morgan D. Bazilian, Nicholas Wagner, and Ricardo Gorini. "The role of renewable energy in the global energy transformation." *Energy Strategy Reviews* 24 (2019): 38-50. https://doi.org/10.1016/j.esr.2019.01.006

[3] Yahya, Noor Fateen Afikah, Negar Dasineh Khiavi, and Norahim Ibrahim. "Green electricity production by Epipremnum Aureum and bacteria in plant microbial fuel cell." *Journal of Advanced Research in Applied Sciences and Engineering Technology* 5, no. 1 (2016): 22-31.

[4] Paradiso, Joseph A., and Thad Starner. "Energy scavenging for mobile and wireless electronics." *IEEE Pervasive Computing* 4, no. 1 (2005): 18-27. https://doi.org/10.1109/MPRV.2005.9

[5] Beeby, S. P., M. J. Tudor, and N. M. White. "Energy harvesting vibration sources for microsystems applications." *Measurement Science and Technology* 17, no. 12 (2006): R175. https://doi.org/10.1088/0957-0233/17/12/R01

[6] Anton, Steven R., and Henry A. Sodano. "A review of power harvesting using piezoelectric materials (2003-2006)." *Smart Materials and Structures* 16, no. 3 (2007): R1. https://doi.org/10.1088/0964-1726/16/3/R01

[7] Mitcheson, Paul D., Eric M. Yeatman, G. Kondala Rao, Andrew S. Holmes, and Tim C. Green. "Energy harvesting from human and machine motion for wireless electronic devices." *Proceedings of the IEEE* 96, no. 9 (2008): 1457-1486. https://doi.org/10.1109/JPROC.2008.927494

[8] Wang, Zhong Lin. "Nanogenerators for self-powered devices and systems." *Atlanta, USA: Georgia Institute of Technology* (2011).

[9] Xu, Sheng, Yong Qin, Chen Xu, Yaguang Wei, Rusen Yang, and Zhong Lin Wang. "Self-powered nanowire devices." *Nature Nanotechnology* 5, no. 5 (2010): 366-373. https://doi.org/10.1038/nnano.2010.46

[10] Hu, Youfan, Yan Zhang, Chen Xu, Long Lin, Robert L. Snyder, and Zhong Lin Wang. "Self-powered system with wireless data transmission." *Nano Letters* 11, no. 6 (2011): 2572-2577. https://doi.org/10.1021/nl201505c

[11] Wang, Zhong Lin, and Jinhui Song. "Piezoelectric nanogenerators based on zinc oxide nanowire arrays." *Science* 312, no. 5771 (2006): 242-246. https://doi.org/10.1126/science.1124005

[12] Fan, Feng-Ru, Zhong-Qun Tian, and Zhong Lin Wang. "Flexible triboelectric generator." *Nano Energy* 1, no. 2 (2012): 328-334. https://doi.org/10.1016/j.nanoen.2012.01.004

[13] Dharmasena, RD Ishara G., Jonathan HB Deane, and S. Ravi P. Silva. "Nature of power generation and output optimization criteria for triboelectric nanogenerators." *Advanced Energy Materials* 8, no. 31 (2018): 1802190. https://doi.org/10.1002/aenm.201802190

[14] Zhang, Renyun, and Håkan Olin. "Material choices for triboelectric nanogenerators: A critical review." *EcoMat* 2, no. 4 (2020): e12062. https://doi.org/10.1002/eom2.12062

[15] Lin, Hongbin, Minghui He, Qingshen Jing, Weifeng Yang, Shutang Wang, Ying Liu, Yaoli Zhang et al. "Angle-shaped triboelectric nanogenerator for harvesting environmental wind energy." *Nano Energy* 56 (2019): 269-276. https://doi.org/10.1016/j.nanoen.2018.11.037

[16] Wang, Qi, Minfang Chen, Wei Li, Zhen Li, Yantao Chen, and Yongmei Zhai. "Size effect on the output of a miniaturized triboelectric nanogenerator based on superimposed electrode layers." *Nano Energy* 41 (2017): 128-138. https://doi.org/10.1016/j.nanoen.2017.09.030

[17] Byun, Kyung-Eun, Min-Hyun Lee, Yeonchoo Cho, Seung-Geol Nam, Hyeon-Jin Shin, and Seongjun Park. "Potential role of motion for enhancing maximum output energy of triboelectric nanogenerator." *APL Materials* 5, no. 7 (2017). https://doi.org/10.1063/1.4979955

[18] Rostam, Sarkawt, Alan Kareem Ali, and Firdaws Haidar AbdalMuhammad. "Experimental investigation of mechanical properties of PVC polymer under different heating and cooling conditions." *Journal of Engineering* 2016 (2016). https://doi.org/10.1155/2016/3791417
[19] Lewandowski, Krzysztof, and Katarzyna Skórczewska. "A brief review of poly (vinyl chloride)(PVC) recycling." *Polymers* 14, no. 15 (2022): 3035. https://doi.org/10.3390/polym14153035
[20] Zhang, Zhi, Xiongfei Sun, Ying Chen, Dereje Kebebew Debeli, and Jiansheng Guo. "Comprehensive dependence of triboelectric nanogenerator on dielectric thickness and external impact for high electric outputs." *Journal of Applied Physics* 124, no. 4 (2018). https://doi.org/10.1063/1.5031809
[21] Zhang, Xu-Wu, Gui-Zhong Li, Gui-Gen Wang, Ji-Li Tian, Yi-Lin Liu, Da-Ming Ye, Zheng Liu, Hua-Yu Zhang, and Jie-Cai Han. "High-performance triboelectric nanogenerator with double-surface shape-complementary microstructures prepared by using simple sandpaper templates." *ACS Sustainable Chemistry & Engineering* 6, no. 2 (2018): 2283-2291. https://doi.org/10.1021/acssuschemeng.7b03745
[22] Zhou, Qitao, Shuwen Chen, Jianxin Lai, Shujun Deng, Jing Pan, Jeong Min Baik, and Fan Xia. "High rotational speed hand-powered triboelectric nanogenerator toward a battery-free point-of-care detection system." *RSC Advances* 11, no. 38 (2021): 23221-23227. https://doi.org/10.1039/D1RA03323A
[23] Hong, Daewoong, Jungho Choe, Yongjoo Lee, and Jaehwa Jeong. "Test bed for rotation-based triboelectric nanogenerators." *Review of Scientific Instruments* 91, no. 3 (2020). https://doi.org/10.1063/1.5141487
[24] Chandrasekhar, Arunkumar, Venkateswaran Vivekananthan, Gaurav Khandelwal, and Sang Jae Kim. "A fully packed water-proof, humidity resistant triboelectric nanogenerator for transmitting Morse code." *Nano Energy* 60 (2019): 850-856. https://doi.org/10.1016/j.nanoen.2019.04.004
[25] Gomes, A., C. Rodrigues, A. M. Pereira, and J. Ventura. "Influence of thickness and contact area on the performance of pdms-based triboelectric nanogenerators." *arXiv preprint arXiv:1803.10070* (2018).